Journal of ELECTRICAL ENGINEERING, VOL. 53, NO. 11-12, 2002, 299–307

ANALYTICAL, NUMERICAL AND EXPERIMENTAL ANALYSIS OF THE RISE OF TEMPERATURE OF ENCASED CONDUCTORS: PART I

František Janíček — Justín Murín — Jaroslav Lelák [*]
Zoltán Harsanyi [**]

The first part of this article deals with the computational analysis of the temperature rise of encased conductors of a nuclear power plant in the steady state. The generated heat is due to electric losses in different modes of loading. In the second part of this article the results of these computations (by analytical and finite element method) are compared with the results of an experiment performed on a one-phase model of an encased conductor. The obtained results are useful in assessing the safety of operation of conductors in the operating mode and of the possible critical states of the power plant.

K e y w o r d s: encased conductor, temperature rise, nuclear power plant, computation and experiment

1 INTRODUCTION

Electric power plants, both classical and nuclear, are complex aggregates of machinery, electric, and controlling systems. The safety of operation of these systems depends on reliable operation of every single component. As for the need to satisfy the requirements imposed from the operation states, an important role belongs to interconnections by encapsulated conductors. The electrical and mechanical strengths as well as other properties and parameters of encapsulated conductors must not only ensure the transfer of the designed load in the nominal mode but also a certain current margin for the case of critical or emergency states [1–3].

In technical practice, diverse types of encapsulated conductors are used, most often conductors with divided (split) casings and with longitudinally interconnected casings [46]. The encapsulated conductors with divided casings are electrically insulated from each other. Their advantage is that no eddy currents are induced in them. Hence, the total electric losses and internal heat sources resulting from them are lower. The casings provide perfect protection in the region of high density of electric energy. Their drawback is that the eddy currents shield the external magnetic fields only partially, therefore losses into the ambient occur in normal operation and in the case of short connections strong electromagnetic forces act between the conductors of single phases.

Eddy currents induced in single segments of the casing are distributed along the perimeter non-symmetrically giving rise to an uneven distribution of temperature both on the perimeter and along the casing. The encased conductors with interconnected casings are electrically connected by welded joints along the whole length, and grounded on both sides. Since the casing with the conductor represents an instrument transformer with transformation ratio $1 : 1$, currents are induced in the casing approximately equal to those in the conductor and phase shifted by $180°$. These currents eliminate the external magnetic field and short-circuit forces. No losses into the ambient occur and, hence, no warming of the nearby metallic constructions. The losses are practically the same in all phases and due to equal currents in the conductor and in the casing there are no eddy currents in the casing and, consequently, no temperature gradients between different cross-sections of the conductor. The system conductor-casing is stiffer and, hereby, mechanically more resistant. The drawback is that the longitudinal currents in the casing result in considerable losses in the casing approximately equal to those in the conductor. This is manifested by an increased rise of temperature as compared with divided casings.

The warming of encased conductors markedly affects the economy and safety of transmission of electric energy. The solution of the temperature field of EC is therefore an important and complex issue of heat transfer taking place in an internal source due to electric losses. In the contribution we present a complex method of assessing the rise of temperature of ECs by two computational methods and by an experiment. After defining the starting conditions and presumptions we build a thermo-mechanical model of EC for computing the stationary temperature field caused by electric losses and its transfer into the ambient by conduction, convection, and radiation. The task is resolved by classical approaches of thermo-kinetics as well as by the finite element method (FEM). To verify the results of

[*] Slovak University of Technology, Faculty of Electrical Engineering and Information Technology Bratsialava, Department of Power Engineering (F.J.), Department of Mechanics (J.M.), Department of Electrotechnology (J.L.)

[**] Nuclear Power Plants Research Institute Trnava

ISSN 1335-3632

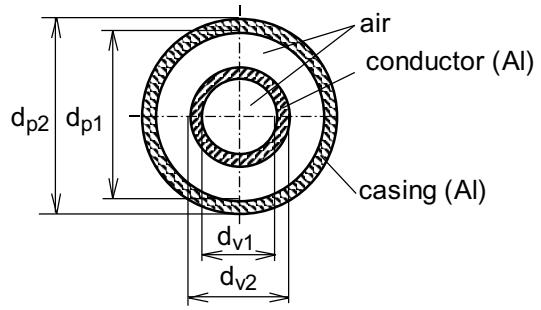

Fig. 1. Cross-section of an encapsulated conductor.

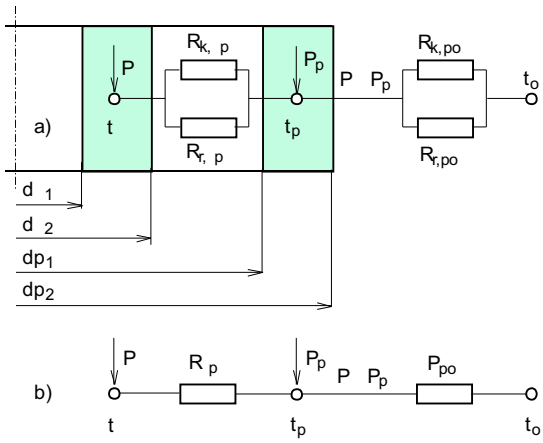

Fig. 2. Equivalent thermal scheme of the encased conductor.

computation, an experiment was performed by measuring the warming of a 2.5 kA encased conductor. In addition to measuring the temperature in the stationary state, measurement was conducted also for non-stationary current load states. The results of computations are presented in graphs and in the second part of this article they are compared with experimental data. In order to resolve the problem comprehensively, also such operation factors are analyzed as the current in the casing, emissivity of the surface of the EC, and ambient temperature. These factors affect the rise of temperature of ECs most strongly. The computations were performed for 2.5 kA and 4 kA encased conductors [7].

2 ANALYTICAL METHOD FOR CALCULATING THE WARMING–UP OF ENCAPSULATED CONDUCTORS IN STATIONARY STATE

2.1 Presuppositions and construction of equations for calculating the temperature rise of the conductor and casing

The fundamental presupposition is the existence of an infinitely long, in every cross- section equally and in the radial direction symmetrically loaded encapsulated conductor. This presupposition allows solving this generally 3D problem as a 2D problem of the temperature field in the cross-section of the EC shown in Fig. 1.

To build the heat transfer equations in the cross-section of the EC we use the equivalent thermal scheme shown in Fig. 2 and the following presuppositions:

- the source of heat consists only of electrical losses in the conductor and in the casing which remain the same in all cross-sections along the whole length of the conductor,
- the generated heat is transferred from the conductor and the casing in the radial direction only,
- due to the small thickness of the walls of the conductor and of the casing, their thermal resistance for heat conduction is negligible,
- in the air gap between the conductor and the casing (limited convection), heat is transferred by conduction with equivalent thermal conductivity,
- between the outer surface of the conductor and the inner surface of the casing, heat is exchanged by radiation,
- heat is transferred from the outer surface of the casing into the ambient by free convection and by radiation,
- the formulae for calculating the electric losses account for the skin effect as well as the effect of mutual proximity of conductors of different phases,
- the all material parameters are temperature dependent, thus we consider a non-linear heat transfer.

In the encased conductor, losses are generated in the conductor, P_v, and in the casing, P_p [W/m]. Losses P_v are transferred from the conductor into the casing by convection and radiation, and similarly losses $P_p + P_v$ are transferred from the surface of the casing into the ambient.

From the simplified equivalent scheme shown in Figs. 2a and 2b, the following relations result for the temperature rise of the casing, Δt_p, and of the conductor, Δt_v:

$$\Delta t_p = t_p - t_o = (P_v + P_p)\, R_{po} \qquad [°C] \quad (1)$$

$$\Delta t_v = t_v - t_o = P_v R_{vp} + (P_v + P_p)\, R_{po} \qquad [°C] \quad (2)$$

Here, R_{po} is the thermal resistance between the casing and the ambient, R_{vp} is the thermal resistance between the conductor and the casing, t_o is the ambient temperature, t_v is the temperature of the conductor, and t_p is the temperature of the casing.

2.2 Calculation of thermal resistances

To calculate the thermal resistances, standard formulae have been used as described in [8, 9]. Here we will only describe the procedure of calculating the equivalent conductivity of air in the air gap between the casing and the conductor, and the calculation of the coefficient of heat transfer by convection from the surface of the casing into the ambient.

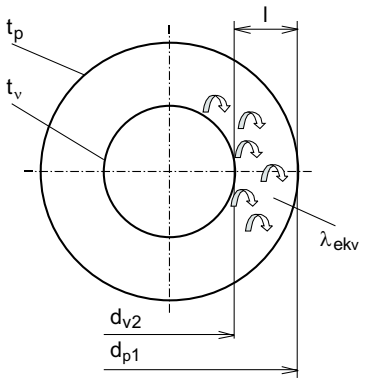

Fig. 3. Limited heat convection.

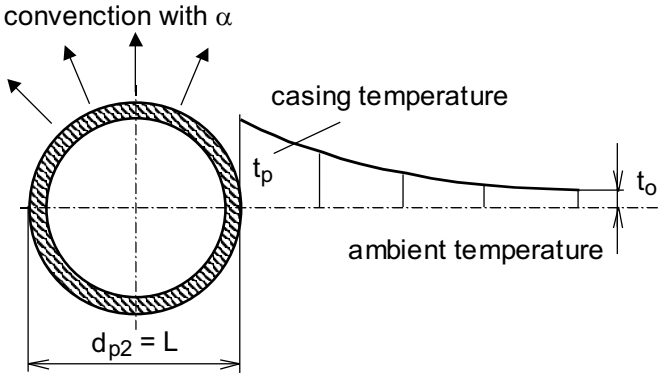

Fig. 4. Free heat convection from the surface of the casing

2.2.1 Calculation of the equivalent conductivity of air

Limited heat convection occurs in the air gap between the outer surface of the conductor and the inner surface of the casing.

Since the calculation of the coefficient of convection between the two surfaces is difficult, the limited heat convection is replaced by heat conduction whereas the conductivity of air is replaced by equivalent conductivity λ_{ekv} which accounts also for the heat removal by convection (Fig. 3).

The equivalent air conductivity reads [10]

$$\lambda_{\mathrm{ekv}} = \lambda \varepsilon_k \qquad [\mathrm{W/mK}], \tag{3}$$

where the heat conductivity of air (similarly like kinematic viscosity $\upsilon\,[\mathrm{m^2/s}]$ and the Prandtl number Pr [–]) depend on the average temperature (see [17])

$$t = \frac{t_v + t_p}{2} \qquad [^\circ\mathrm{C}]\,. \tag{4}$$

Then the thermal expansivity of air is

$$\beta = \frac{1}{273 + t} \qquad [1/\mathrm{K}]\,. \tag{5}$$

By making use of the experimental data given in [17] and of the code in [12], the temperature dependences of λ, υ and Pr can be converted into continuous functional dependences. Then the Grasshoff number is

$$Gr = \frac{g\beta\,(t_v - t_p)\,l^3}{\upsilon^2}\,, \tag{6}$$

where $g = 9.81\,[\mathrm{m/s^2}]$ is the acceleration of gravity and $l = (dp_1 - dv_2)/2$ [m]is the thickness of the air gap.

Calculation of the coefficient of limited convection ε_k is based on criterial equations the form of which depends on the product $Gr\,Pr$ [13]

$$10^3 < Gr\,Pr < 10^6 \qquad \varepsilon_k = 0.105(Gr\,Pr)^{0.3} \tag{7}$$

$$10^6 < Gr\,Pr < 10^{10} \qquad \varepsilon_k = 0.40(Gr\,Pr)^{0.2} \tag{8}$$

$$Gr\,Pr < 10^{10} \qquad \varepsilon_k = 1 \tag{9}$$

Since these formulae contain unknown temperatures of the casing and conductor, the problem is non-linear and must be solved iteratively.

Table 1. Coefficients needed to calculate the Nusselt number Nu.

$Gr\,Pr$	c	n
10^{-3}–5×10^2	1.18	1/8
5×10^2–2×10^7	0.54	1/4
2×10^7–10^{13}	0.135	1/3
$Gr\,Pr < 10^{-3}$	$Nu = 0.5 = \mathrm{const}$	

2.2.2 Calculation of heat transfer by convection from the surface of the casing into the ambient

We will assume axially symmetrical heat removal by convection, as depicted in Fig. 4.

The coefficient of heat transfer can be found from the criterial equation [13]

$$\alpha = \frac{Nu\lambda}{L} \qquad [\mathrm{W/m^2K}]\,, \tag{10}$$

where $L = dp_2\,[\mathrm{m}]$, λ is the thermal conductivity of air depending on the average temperature $t = (t_p + t_o)/2\,[^\circ\mathrm{C}]$, and $Nu = c(Gr\,Pr)^n$ is the Nusselt number. Quantities c and n depend on the value of the product of the Grasshoff and Prandtl numbers (see Tab. 1) [13].

Also here it is necessary to consider the dependence of quantities λ, υ and Pr on the average temperature $t\,[^\circ\mathrm{C}]$.

If the thermal expansivity of the ambient air is expressed as

$$\beta = \frac{1}{273 + t} \qquad [1/\mathrm{K}]\,,$$

then the Grasshoff number is

$$Gr = \frac{g\beta(t_p - t_o)\,l^3}{\upsilon^2}\,. \tag{11}$$

By considering Tab. 1, from eqn. (10) one can find the coefficient of convection. Since the casing temperature t_p is unknown, α must be calculated iteratively.

2.2.3 Evaluation of heat sources in the conductor and casing

The internal sources of heat in the encapsulated conductor are due to electric losses. Their evaluation depends on the type of encased conductor and it is inevitable to evaluate them separately for the conductor and the casing.

a) Heat power of the conductor

In every conductor carrying current I_v a loss power is created (per unit length)

$$P_v = R_v I_v^2 \quad [\mathrm{W/m}]\,, \tag{12}$$

where R_v is the resistance of the conductor depending primarily on the temperature of the conductor t_v [°C]. In the case of AC current, however, the resistance may be affected also by other factors such as skin effect, proximity effect, *etc*. At temperatures well below the melting point of the conducting material the resistance of the conductor grows linearly with temperature and is calculated as [14]

$$R_v = R_{20v}\big(1 + \alpha_R(t_v - 20)\big)\, k_{skinv} \quad [\Omega/\mathrm{m}]\ , \tag{13}$$

where R_{20v} is the resistance of the conductor at 20 °C,

$$R_{20v} = \rho_{20}\frac{1}{S_v} \quad [\Omega/\mathrm{m}]\ , \tag{14}$$

ρ_{20} [Ωm] is the resistivity of the conductor at 20 °C, α_R [1/K] is the linear temperature resistance coefficient, and S_v [m^2] is the cross-sectional area of the conductor. The skin effect coefficient can be obtained from diagrams and for small widths of the annulus of the conductor and casing it does not manifest itself markedly, this means that $k_{skinv} = 1$ [15]. The proximity effect is considered in such cases only when the ratio of distances of two neighbouring conductors (in multiphase arrangements of the conductors) and of the conductor diameter is equal or smaller than 4 [15].

b) Heat power of the casing

The heat power consists of losses due to eddy currents and of losses due to longitudinal currents.

The ratio of longitudinal and conductor current depends on the type of grounding of the casing. For casings split into short and unilaterally grounded segments the current in the casing is $I_p = (15 - 20\%)I_v$.

For losses due to eddy currents Conagla [14] gives the formula

$$P_w = 1.04 R_p \Big(\frac{dp_2}{d_{vz}}\Big)^{2.13}(I_v - I_p)^2 \quad [\mathrm{W/m}]\,, \tag{15}$$

where R_p is the resistance of the casing at 50 Hz and operating temperature t_p, dp_2 is the outer diameter of the casing [m], and d_{vz} is the distance between the centres of two neighbouring encased conductors [m].

The electric resistance of the casing is given similarly like for the conductor, thus

$$R_p = R_{20p}\big(1 + \alpha_R(t_p - 20)\big)\, k_{skinp} \quad [\Omega/\mathrm{m}]\,, \tag{16}$$

where $R_{20p} = \rho_{20}\frac{1}{S_p}$ [Ω/m] is the resistance of the casing at 20 °C. The total heat power is then given as a sum of the losses due to eddy and longitudinal currents

$$P_p = P_w + R_p I_p^2 \quad [\mathrm{W/m}]\,. \tag{17}$$

The skin effect for the casing is described in a similar way like for the conductor [15].

2.2.4 Computer code for computing the temperature rise of the conductor and casing compiled by software package Mathematica

The derived formulas for the warming of the encased conductor have been used to develop a code by Mathematica [12] that can be divided into the following parts:

1. Reading the tabulated data for kinematic viscosity v and heat conductivity of air λ as functions of temperature, creating linear interpolations between respective tabulated data given in [11].
2. Defining the entries — in this part the following parameters are entered:
   - inner and outer diameters of the conductor and casing,
   - length parameter L needed to calculate the coefficient α,
   - length parameter l needed to calculate the coefficient λ_{ekv},
   - emissivities of the surfaces of the conductor and of the casing,
   - ambient temperature,
   - current flowing in the conductor,
   - expression defining the ratio between the currents in the conductor and in the casing.
3. Defining the formula for calculating the coefficient of convection, α between the casing and ambient.
4. Defining the formula to calculate the coefficient of equivalent heat conductivity of air, λ_{ekv}, between the outer surface of the conductor and the inner surface of the casing.
5. Defining the formula for the replacement emissivity for the outer surface of the conductor and the inner surface of the casing.
6. Defining and merging single thermal resistances.
7. Defining the formulae for heat sources in the conductor and casing as functions of the currents flowing in the conductor and casing.
8. Compiling and solving a system of two non-linear equations, the temperatures of conductor and casing being unknown quantities.
9. Printing the calculated thermo-physical parameters and the computed temperatures of the conductor and casing.

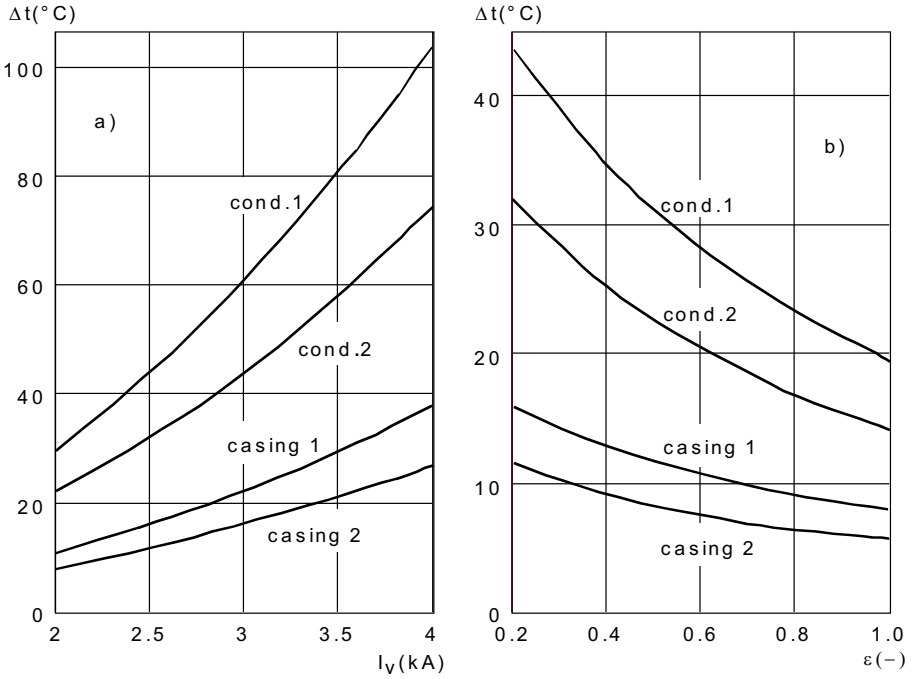

Fig. 5. Warming of the encased conductor in dependence on the current I_v, and the emissivity.

Comments on some parts of computation:

Item 3:
When entering the formula for calculating the coefficient α one must enter different forms of this relation for different values of the product of parameters Gr and Pr. Parameter Pr is constant in the studied temperature range but Gr is a function of casing and ambient temperatures.

Item 4:
When calculating λ_{ekv}, first the convection coefficient ε_k is to be evaluated expressing the effect of convection upon the heat transfer between the conductor and casing. The form of this parameter also depends on the product of Gr and Pr. Here, however, Gr is a function of conductor and casing temperatures.

Item 7:
The solution of the system of two non-linear equations, in which the conductor and casing temperatures are unknowns, is performed by an internal subroutine implemented in Mathematica. This subroutine employs the Newton iterative method. Since this is a numerical rather than analytical solution of a non-linear system of equations, the subroutine requires that the user define the initial parameters to find a correct solution for each unknown. In the case of an inappropriate choice of these initial parameters the system need not converge to the correct solution; the code returns a remainder. One can begin, *eg*, with taking the standards of admissible temperatures of the conductor and casing.

2.2.5 Numerical experiment

The objective of our computations by the analytical method handled by Mathematica was to evaluate the warming of 2.5 kA and 4 kA encased conductors in dependence on the current flowing through the conductor, I_v. Both types of encased conductors have the same outer diameters of the casing and conductor ($dp_2 = 0.270$ m, $d_{v2} = 0.132$ m) and differ just in the thicknesses of the walls. The 2.5 kA conductor has a 11 mm thick wall of the conductor and 5 mm thick wall of the casing. In the 4 kA conductor, the wall thickness of the conductor is 16 mm, whereas that of the casing is 8 mm. Both the conductor and the casing are made of aluminium with thermal conductivity $\lambda = 229.1$ W/mK and resistivity $\rho_{20} = 2.8 \times 10^{-8}\,\Omega$m at 20 °C. The linear temperature coefficient of resistance is 0.0037 1/K.

Since the temperature rise of the encased conductor depends on a number of other parameters, we have chosen their constant values: current through the casing $I_p = 0.2\,I_v$, ambient temperature $t_o = 30$ °C, emissivity of outer and inner surfaces of the conductor and casing $\varepsilon_v = \varepsilon_p = 0.2$, mutual distance of two neighbouring phases $d_{vz} = 0.35$ m. As the wall thicknesses of the encased conductor are small, we have not consider the skin effect.

Figure 5A shows the dependence of the warming of the 2.5 kA encased conductor — conductor (casing) 1, and for the 4 kA encased conductor — conductor (casing) 2 in dependence on current I_v. As expected, the rise of temperature is higher for the 2.5 kA encased conductor. For example, at a current of $I_v = 2.5$ kA the conductor warming is 43.87 °C and casing warming is 16.1 °C. At the same current, the warming of the 4 kA encased conductor is: conductor by 32.08 °C, casing by 11.67 °C. Generally, the warming of the 2.5 kA conductor is higher by 30 to 40 % as compared with that of the 4 kA encased conductor.

Figure 5B shows the effect of emissivity upon the warming of the encased conductor at a current of $I_v = 2.5$ kA. All other parameters of the computer model are identical with the previous experiment. One can see that the growing emissivity of the surfaces of the encased conductor has a significant effect upon lowering the temperature rise of both the conductor and casing.

3 NUMERICAL ANALYSIS OF WARMING OF ENCASED CONDUCTORS BY THE FINITE ELEMENT METHOD

The finite element method (FEM) is a computer-oriented numerical procedure for solving the problems of the field theory (force, strain, velocity, acoustic, electric, electromagnetic, weakly or strongly coupled, and other problems). By means of discretizing the definition region of the functionals of a tensor field into sub-regions, finite elements defined by a selectable number of nodal points, the problem of finding depending variables of the field in an infinite number of points is replaced by calculating the field unknowns in a finite number of nodal points.

The fundamental (governing) field equations (usually this is a system of partial differential equations) are discretized and converted into a linear (or non-linear) algebraic system of equations for calculating the unknowns of the field in the nodal points. Based on the values of the field in the nodal points one can then evaluate the field values at any point in the studied region by means of "shape functions".

As for the shape of the discretized region, the finite elements may be of line, surface or volume types. The nodal points through which all inter-element bonds are transferred lie in the vertices of the finite element but for more precise modelling of the region they can also lie in the middles of edges or in the centres of gravity of the areas or volumes of the finite elements. With making the grid of finite elements finer the computation of the field unknowns becomes more accurate.

The surface of the body (which may also be multiply continuous) can be divided into parts (they may even overlap): part S_1 with prescribed temperature, part S_2 with prescribed heat delivery (or removal) by conduction, part S_3 with prescribed head removal (or delivery) by convection. From part S_4 of the surface, heat may be removed by radiation.

The problem of heat transfer in the three-dimensional body with volume V is described by the functional [5], which satisfies the boundary conditions

$$I = \frac{1}{2}\int_V \Big[\lambda_x\Big(\frac{\partial T}{\partial x}\Big)^2 + \lambda_y\Big(\frac{\partial T}{\partial y}\Big)^2 + \lambda_z\Big(\frac{\partial T}{\partial z}\Big)^2 - 2\Big(\dot q - \rho c\frac{\partial T}{\partial \tau}\Big)T\Big]\,\mathrm{d}V + \int_{S_2} qT\,\mathrm{d}S_2 + \frac{1}{2}\int_{S_3}\alpha(T-T_o)^2\mathrm{d}S_3 \quad [\mathrm{WK}] \tag{18}$$

where λ_x, λ_y, λ_z are the thermal conductivities of the material in respective directions [W/mK],

$T = T(x, y, z, \tau)$ is the temperature field searched for [K],

$\dot q$ is the internal source of heat [W/m^3],

ρ is the material density [kg/m^3],

c is the specific heat [J/kgK],

q is the heat flux [W/m^2] delivered (removed) through surface S_2,

α is the coefficient of heat transfer by convection [W/m^{2}K] through surface S_3 with ambient temperature T_o [K].

Functional (18) describing the heat transfer through the whole region can be replaced by a sum of functionals of the same type for single finite elements I^e

$$I = \sum_e I^e\,. \tag{19}$$

By minimizing the functional (19) one can get an algebraic system of equations for the unknown, time dependent temperature field.

For the sake of simplicity, formulation of the fundamental FEM equations for numerical calculation of the temperature field will be presented only for two-dimensional problems.

3.1 Formulation of FEM equations for a plane steady state problem of heat transfer

The planar part with surface area S, volume V and unit thickness h lie in the x, y plane and is divided into finite elements. A selected element (*eg* bilinear triangular) has a volume $V^e = S^e 1\,[\mathrm{m}^3]$, where $S^e\,[\mathrm{m}^2]$ is a plane surface of the element defined by nodal points 1,2,3. The surface of the element in the direction of its thickness can theoretically be divided into three parts (Fig. 6):

$S_1^e = s_1^e 1 = s_1^e$ [m^2] is the part of the surface of the element with prescribed temperature,

$S_2^e = s_2^e 1 = s_2^e$ [m^2] is the part of the element surface through which heat is delivered (removed) by conduction,

$S_3^e = s_3^e 1 = s_3^e$ [m^2] is the part of the element surface where convection takes place.

To describe the stationary plane heat transfer within the selected finite element with two boundary conditions, functional (18) reads

$$I^e = \frac{1}{2}\int_{V^e}\Big[\lambda_x\Big(\frac{\partial T^e}{\partial x}\Big)^2 + \lambda_y\Big(\frac{\partial T^e}{\partial y}\Big)^2 - 2\dot q T^e\Big]\mathrm{d}V + \int_{S_2^e} qT^e\mathrm{d}S_2 + \frac{1}{2}\int_{S_3^e}\alpha\Big(T^e - T_o\Big)^2\mathrm{d}S_3 \tag{20}$$

where T^e is the unknown temperature field on finite element e. If the material is isotropic, then the thermal conductivities are $\lambda_x = \lambda_y = \lambda$. Let us assume that

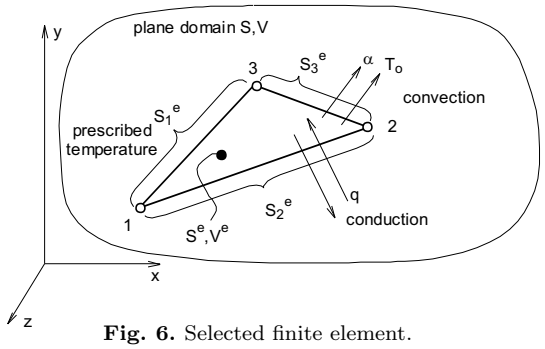

Fig. 6. Selected finite element.

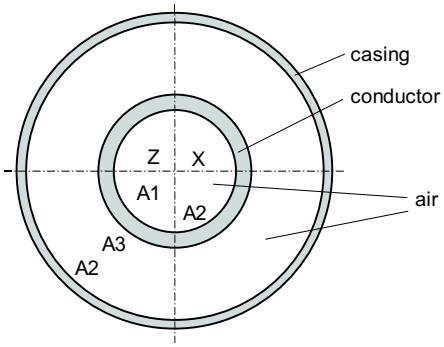

Fig. 7. Cross-section of the encased conductor.

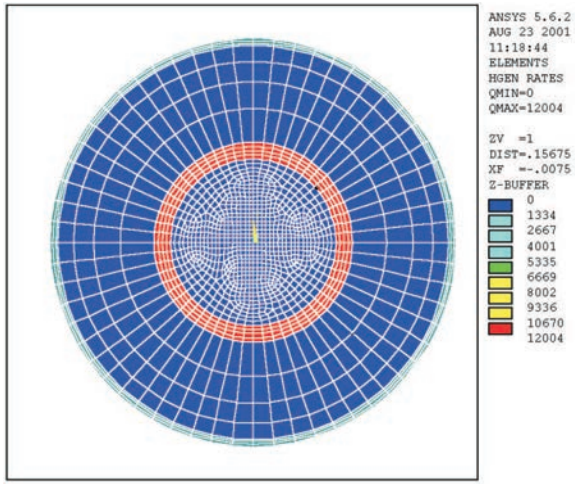

Fig. 8. The mesh of finite elements PLANE77,the generated heat.

the temperature in an arbitrary point of the element is a function of its position and of the temperatures at nodal points T_i^e, $(i = 1, 2, 3)$. Then

$$T^e = N_1 T_1^e + N_2 T_2^e + N_3 T_3^e = \sum_i N_i T_i^e \qquad (21)$$

and $N_i = N_i(x, y)$ are the shape functions. As a rule, these are polynomials (their order depends on the number of nodal points of the finite element).

An algebraic system of equations to retrieve the temperatures in the nodal points is obtained by minimizing the functional (18) or (20) and the system has a matrix form

$$(\mathbf{K}_1^e + \mathbf{K}_2^e)\,\mathbf{T}^e = \mathbf{P}_1^e - \mathbf{P}_2^e + \mathbf{P}_3^e\,, \qquad (22)$$

where

- $\mathbf{K}_1^e$ is the matrix of thermal conductivity,
- $\mathbf{K}_2^e$ is the matrix of convection,
- $\mathbf{P}_1^e$ is the vector of heat sources transformed into the nodal points,
- $\mathbf{P}_2^e$ is the vector of heat supplied (or removed) by conduction,
- $\mathbf{P}_3^e$ is the vector of heat supplied (or removed) by convection.

Particular forms of these matrices and vectors for a bilinear planar triangular finite element as well as for other types of element can be found, *eg*, in [16].

For the whole region discretized into finite elements we get an algebraic set of equations in the form

$$(\mathbf{K}_1 + \mathbf{K}_2)\mathbf{T} = \mathbf{P}_1 - \mathbf{P}_2 + \mathbf{P}_3\,. \qquad (23)$$

The meaning of matrices and vectors in (23) is the same like in the element equation (22). The difference is that eqn. (23) applies to the whole discretized region, thus it represents a set of equations for the unknown temperature field in all nodal points of the region. Single matrices and vectors on the right sides are obtained in the usual way as a sum of extended forms for all finite elements [16, 17].

The global matrices of system (23) are symmetrical, which allows employing the simplest and most efficient methods to solve the system.

The involvement of the boundary condition for heat transfer by radiation from a part of the body surface, S_4, into the FEM equations gives rise to the matrix of radiation $\mathbf{K}_4$ and vector of radiation $\mathbf{P}_4$ composed of elemental matrices of radiation, $\mathbf{K}_4^e$, and vectors of radiation, $\mathbf{P}_4^e$, where

$$\mathbf{K}_4^e \equiv \int_{s_4^e} h N_i N_j \mathrm{d}s_4^e\,, \quad \mathbf{P}_4^e \equiv \int_{s_4^e} h T_o \mathrm{d}s_4^e\,. \qquad (24)$$

There is introduced a quasiconstant coefficient of radiation [16]

$$h = \sigma\varepsilon(T^{e2} - T_o^2)(T^e - T_o)\,, \qquad (25)$$

where σ is the Stephan-Boltzmann constant and ε is the emissivity of the surface radiating heat.

Since coefficient h in fact depends on the unknown temperature, the set of equations (23) completed with (24) must be solved iteratively [16, 18].

3.2 NUMERICAL RESULTS OF OBTAINED BY FEM

From the point of view of FEM, the solution of the stationary temperature state in an encased conductor means to solve a stationary plane problem of heat transfer with

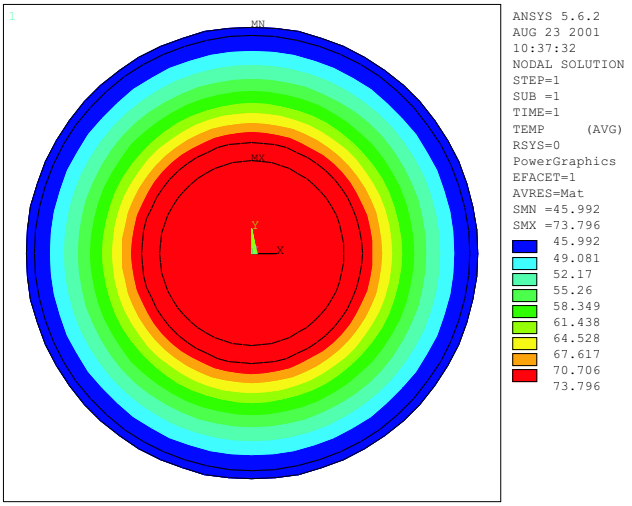

Fig. 9. The temperature field obtained by FEM.

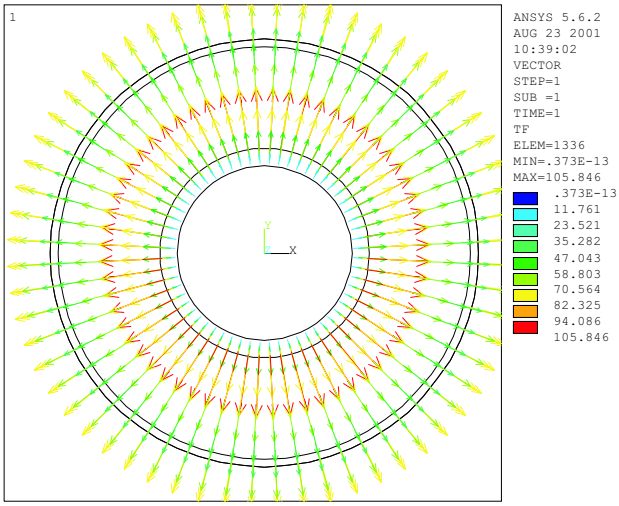

Fig. 10. The heat flux obtained by FEM.

internal heat sources assuming that heat propagates uniformly in radial directions. Figure 7 shows a cross-section of the encased conductor showing the conductor itself, the casing, air gaps inside the conductor and between the conductor and the casing. Heat is generated in both the conductor and casing and transferred by conduction (unlike in the equivalent scheme of the analytical solution, in the FEM model we have accounted also for heat transfer by conduction through the walls of the conductor and of the casing), radiation and limited convection to the surface of the casing from which the heat is removed by free convection and radiation into the ambient air.

For the same geometrical and material parameters like in the analytical solution, we have created a FEM model. To model the cross-section surfaces of the conductor, casing, and the two air gaps we used an 8-point isoparametric plane finite element PLANE77 of the software package ANSYS [19]. For the air inside the conductor, we used thermal conductivity of $\lambda = 0.029\,\mathrm{W/mK}$. The problem of heat radiation from the two surfaces of the conductor and from the two surfaces of the casing was modelled by elements LINK32 and by superelement MATRIX50. The grid of finite elements along with given sources of heat is shown in Fig. 8. The generated heat in the conductor is $\dot{q}_v = P_v/S_v = 12003.7\,\mathrm{W/m^3}$, the generated heat in the casing is $\dot{q}_p = P_p/S_p = 4682.9\,\mathrm{W/m^3}$.

Figure 9 shows the found temperature field in single parts of the cross-section. Figure 10 shows the corresponding heat flux. It is evident from these figures that the rise of temperature is highest for the conductor and for the air contained herein, their temperature being $t_v = 73.79\,^\circ\mathrm{C}$. Then the temperature monotonically decreases to the surface of the casing. This has a temperature of $t_p = 45.99\,^\circ\mathrm{C}$. The warming of the conductor is $\Delta t_v = 43.79\,^\circ\mathrm{C}$, the warming of the casing is $\Delta t_p = 15.99\,^\circ\mathrm{C}$ (corresponding temperature of the conductor or casing minus ambient temperature).

Comparison of the analytical solution and the numerical solution by FEM reveals very good agreement of the results. The slight difference (hundredths of °C) may be due to the fact that the FEM model includes heat conduction through the materials of the conductor and casing as well as conduction through the air enclosed inside the conductor. We have also included heat radiation from the inner surface of the conductor. The FEM model, as compared with the analytical solution, is more complete and accurate, hence the results are believed to be trustworthier.

4 CONCLUSION

This first part of our contribution describes the procedure of computational verification of the warm-up of encased conductors feeding the internal consumption of the nuclear power plant. The obtained results provide sufficient information on thermal loading of encased conductors in different operating states. The good match of the computed results obtained using both the analytical and finite element methods proves the trustworthiness and correctness of the performed analyses. Experimental assessment of these problems has been carried out too, and we briefly describe it in the second part of our contribution [20].

The achieved results can be utilized to assess the possible risks of current loading of encased conductors due to heat stresses. Based on the knowledge of the critical values of heat stresses it is possible to conduct strength and deformation analyses and to evaluate potential effects

of the warm-up upon the system of encased conductors. Detailed material analysis of single components of the encased conductor may reveal potential dangers also from the point of view of electrical loading.

Acknowledgements

Research supported by VEGA-grant 1/7604/20.

References

[1] STN 38 1120 Vlastná spotreba tepelných elektrární a teplární. Bratislava, SÚTN 1995. (in Slovak)

[2] JANÍČEK, F.: Zabezpečenie vlastnej spotreby elektrární počas beznapäťového stavu elektrizačnej sústavy SR, Habilitačná práca, Bratislava, FEI STU august 1998. (in Slovak)

[3] KROŠLÁK, F.—BELÁŇ, A.—BÍZIK, J.–FECKO, Š.–CHLADNÝ, V.—JANÍČEK, F.—HARSÁNYI, L.—KOLCUN, M.—MUDRONČÍK, D.—MURGAŠ, J.—REVÁKOVÁ, D.—ŠIMUNEK, P.—VESELÝ, V.: Splnenie podmienok pre paralelnú prevádzku elektrizačnej sústavy Slovenskej republiky a sústavy UCPTE, Správa k ZoD č. 73/06/94. Bratislava, KEE FEI STU 1994. (in Slovak)

[4] Dokumentácia k zapuzdreným vodičom 2,5 kA a 4 kA. EGE České Budějovice, marec 1999. (in Slovak)

[5] BACKÁR, P.—HORNÍK, V.: Záťažové pomery zapuzdrených vodičov rezervného napájania vlastnej spotreby, Časopis EE, ročník 5, mimoriadne číslo — zborník ku konferencii Elektrotechnika a elektroenergetika '99, FEI STU 1999. (in Slovak)

[6] JANÍČEK, F.—MURÍN, J.—LELÁK, J.: The Calculation of the Rise of Temperature of an Enclosed Conductor by the Finite Element Method, In: Proc. of the Conference "Elektrotechnika a elektroenergetika 2001", STU Bratislava, pp. 39–41.

[7] JANÍČEK, F.—MURÍN, J.—KOLLÁR, M.: Electromagnetic and Temperature Field od High Power Hollow-coaxial Conductor, Journal of Electrical Engineering **53** No. 9/s, 84-87, presented at XVI-th Electromagnetic Fields and Materials International Conference, September 11-13, 2002, Bratislava, Slovakia.

[8] JANÍČEK, F. a kol.: Posúdenie prúdovo-tepelných režimov zapuzdrených vodičov napájania vlastnej spotreby jadrovej elektrárne Mochovce. Správa k ZoD č. 35/130/01. FEI STU, Bratislava, 2001. (in Slovak)

[9] JANÍČEK, F.—MURÍN, J.—LELÁK, J. Load Condition and Evaluation of the Rise of Temperature in an Enclosed Conductor: J. Electrical Engineering **52** No. 7-8 (2001), 210–216.

[10] MICHEJEV, M.A.: Foundation of Heat Transfer (Osnovy teploperedachi), Energia, Moskva, 1977. (in Russian)

[11] RAŽNJEVIČ, N.J.: Tepelné tabuľky a diagramy, Alfa-SNTL, Bratislava, 1984. (in Slovak)

[12] WOLFRAM, S.: Mathematica — a System for Doing Mathematics by Computer, Adison-Wesley Publishing, Inc., 2001.

[13] KALOUSEK, M.—HUČKO, B.: Heat Transfer (Prenos tepla), STU Bratislava, 1996. (in Slovak)

[14] ELENIČ, P.: Prúdové zaťaženie zapuzdreného vodiča kov-vzduch, Diplomová práca. Katedra elektroenergetiky FEI STU, Bratislava, 2001. (in Slovak)

[15] KALOUSEK, M. a kol.: Oteplenie zapuzdrených vodičov, Katedra mechaniky FEI STU, Bratislava, 1978. (in Slovak)

[16] RAO, S.S.: The Finite Element Method in Engineering, Pergamon press, Oxford, 1982.

[17] McGUIRE, W.—GALLAGHER, R.H.—ZIEMIAN, R.D.: Matrix Structural Analysis, John Wiley and Sons, New York, 2000.

[18] ZIENKIEWICZ, O.C.—TAYLOR, R.L.: The Finite Element Method, Fifth edition, McGraw-Hill Book Company, London, 2000.

[19] ANSYS 5.6. A purpose FEM-program and theory manual. 1999.

[20] JANÍČEK, F.—LELÁK, J.—MURÍN, J.—HARSÁNYI, Z.—HUTTNER, L'. and all.: Analytical, Numerical and Experimental Analysis of the Rise of Temperature of Encased Conductors: Part II., (in preparation).

Received 31 October 2002

František Janíček (Prof, Ing, PhD) graduated in power engineering from the Slovak University of Technology in 1979. In 1984 he gained the PhD degree. In 1999 he was appointed Professor in power engineering. Since 1990 until now he has been a member of the Scientific Council FEI, and since 1995 a member of the Supervisory Board of the Western Slovak Energy Distribution Company. He is the founding member of the Slovak Committee of the World Energy Council. Professor Janíček is the Head Manager of the Project "Qualification of Selected Electric Equipment of the Nuclear Power Plants in Slovakia and in the Czech Republic". Since 2000, Professor Janíček has been the Dean of the Faculty of Electrical Engineering and Information Technology of the Slovak University of Technology in Bratislava.

Justín Murín (Prof, Ing, DrSc) was born in Oravská Lesná in 1951. He graduated from the Slovak University of Technology, Faculty of Mechanical Engineering in 1975. He received PhD degree and DrSc degree in applied mechanics in 1979 and 1994, respectively. In 1987 and 2001 he was appointed Associate Professor and Full Professor. His teaching and research activities include analytical and numerical methods in mechanics and thermomechanics (for instance the solution of both linear and non-linear fields problems by finite element methods).

Jaroslav Lelák (Assoc. Prof, Ing, PhD) was born in Piešťany in 1951. He graduated from the Slovak University of Technology, Faculty of Electrical Engineering in 1974. He received PhD degree in 1985 in Moscow Institute of Power Engineering. In 1996 he was appointed Associate Professor on Department of Electrotechnology. His main field of interest is degradation processes in insulation systems, durability, and reliability of electrical power systems and prophylactic measurements on high voltage equipment. He is reading lectures from subject Optical and metallic cables, Technology of electrical machines and High voltage technique.

Harsányi Zoltán (Ing, PhD) was born in Podunajské Biskupice in 1969. He graduated from the Slovak University of Technology, Faculty of Electrical Engineering in 1992. In 2002 he gained the PhD degree in the branch of Power Engineering. From 1992 to 1997 he worked in Elektrovod Bratislava as a manager of the construction of external power electrical lines. Many of such projects has he implemented abroad, *eg*, in Germany, Slovenia, Czech Republic, and Poland. From 1997 to 2001 he was the general manager of the ZSE š.p. — PS Komárno. Since 2001 he has worked at VÚJE Trnava, a.s. as head of the board of directors. His research activities include the emergency and safety of nuclear power plants.